

Landscape responses to intraplate tectonism: Quantitative constraints from ^{10}Be nuclide abundances

Mark Quigley^{a,*}, Mike Sandiford^a, L. Keith Fifield^b, Abaz Alimanovic^a

^a School of Earth Sciences, The University of Melbourne, VIC 3010, Australia

^b Research School of Physical Sciences and Engineering, Australia National University, Canberra, ACT 0200, Australia

Received 9 March 2007; received in revised form 13 June 2007; accepted 13 June 2007

Available online 22 June 2007

Editor: R.D. van der Hilst

Abstract

Cosmogenic ^{10}Be concentrations in bedrock and alluvium combined with structural studies provide a novel approach for identifying neotectonic forcing of landscape evolution in mildly deforming continental interiors. Measured ^{10}Be concentrations in the Flinders Ranges indicate rapid and spatially variable rates of bedrock erosion in a catchment that has incurred at least three large, surface-rupturing earthquakes since ~ 67 ka. ^{10}Be -derived erosion rates are lower where late Quaternary neotectonic activity is reduced or absent, implying that ^{10}Be concentration may act as a ‘tracer’ for disequilibrium landscapes responding to recent tectonism. Mechanisms for elevated erosion rates include (1) headward migration of fault-generated bedrock knickpoints and resultant oversteepening of stream profiles and catchment hillslopes and (2) liberation of bedrock material from catchment hillslopes via co-seismic shaking. Despite climatic influences on sediment production and transport, this study shows that tectonism can provide a dominant control on bedrock erosion rate and relief production in unglaciated mountain belts, even in intraplate settings where rates of crustal deformation are mild and earthquake activity is episodic.

© 2007 Elsevier B.V. All rights reserved.

Keywords: earthquakes; intraplate tectonics; landscape evolution; ^{10}Be ; cosmogenic; isotopes; erosion

1. Introduction

Concentrations of in situ produced cosmogenic ^{10}Be in bedrock and alluvial sediment provide quantitative measures of surface exposure ages and bedrock and catchment-averaged erosion rates (e.g., Lal, 1991; Granger et al., 1996; Bierman and Steig, 1996; Small et al., 1997; von Blanckenburg, 2006). Spatial distributions of ^{10}Be concentrations therefore provide insight into some of the more pressing problems in landscape

evolution, including quantitative measures of relief development in continental landscapes and the response of landscapes to tectonic and climatic forcing. Recent compilations of world-wide ^{10}Be denudation rates in non-glaciated areas (Riebe et al., 2004; von Blanckenburg, 2006) show a definitive correlation with spatial distributions of tectonic activity, with tectonically active regions characterized by high erosion rates (~ 100 – 1000 m/Myr) and tectonically stable regions characterized by low erosion rates (1–20 m/Myr Bierman and Caffee, 2001, 2002). Conversely, no obvious relationship appears to exist between climate (precipitation and temperature) and ^{10}Be erosion rates (Riebe et al., 2001a,

* Corresponding author.

E-mail address: mquigley@unimelb.edu.au (M. Quigley).

2004; von Blanckenburg, 2006) although some workers have speculated that subtle variations in bedrock erosion rate (on the order of 1–3 m/Myr) may reflect variations in mean annual precipitation (Bierman and Caffee, 2002). Collectively, these studies suggest that spatial variations in the degree of neotectonic forcing of landscapes, via processes such as faulting, knickpoint formation and propagation, and hillslope oversteepening may be recorded by significant variations in ^{10}Be concentrations of bedrock and alluvium derived from these landscapes, while climatic variability may have only a minimal influence on ^{10}Be concentrations (e.g., Riebe et al., 2004).

Cosmogenic ^{10}Be concentrations in bedrock surfaces exposed throughout a landscape also provide point measurements of erosion that can be regionally correlated to assess whether relief has increased (i.e. summit surface erosion outpaced by valley incision), decreased (valley incision outpaced by summit surface erosion) or remained in steady state during the late Quaternary (e.g., Small et al., 1997). The origin of high relief within many intracontinental mountain belts is controversial (Zhang et al., 2001). Some workers have attributed apparent increases in Plio–Quaternary erosion to mild intraplate deformation (Kuhlemann et al., 2001; McMillan et al., 2002; Stock et al., 2005) while others have inferred that erosion rates were increased due to a rapidly oscillating late Cenozoic climate (Zhang et al., 2001). This debate is pertinent to Australia, where relatively high relief (up to 1000 m) apparently ‘youthful’ landscapes have developed in regions subjected to mild rates of intraplate tectonism, with seismic strain rates estimated at 10^{-16} to 10^{-17} s^{-1} (Celerier et al., 2005). The relief characterizing many of Australia’s upland landscapes has been interpreted both as ancient (i.e. pre-Eocene; Veevers, 1984) and as young (i.e. Plio–Quaternary; Callen and Tedford, 1976). In this respect, cosmogenic ^{10}Be dating provides a novel way to distinguish between these competing hypotheses by providing a quantitative measure of whether a landscape is in a state of relief production or decay, and to reconcile this assessment with the tectonic and climatic influences on mountain erosion. Additionally, if ^{10}Be erosion rates are combined with estimates of rock uplift from tectonic studies, estimates of surface uplift, which is of fundamental importance in resolving the dynamics of mountain ranges, may be derived (England and Molnar, 1990).

In this paper, we derive in situ bedrock and catchment-averaged erosion rates from cosmogenic ^{10}Be concentrations in bedrock and alluvium in the semi-arid Flinders Ranges in south-central Australia. The study area has been subjected to a number of

significant, surface-rupturing fault movements since $\sim 80 \text{ ka}$ (Quigley et al., 2006) and therefore provides a setting where ^{10}Be concentrations in a region of mild neotectonic activity can be compared to ^{10}Be concentrations in adjacent, climatically similar settings where such tectonism has not occurred or is occurring at much reduced levels. In addition, in situ erosion rate data is used to characterize relief production and, when combined with structural data, estimate the magnitude of summit surface uplift in the late Quaternary. This allows the geomorphic imprint of intraplate tectonism to be quantified in a continent generally regarded for its tectonic stability, low topography and ancient, slowly eroding landforms (Twidale and Bourne, 1975; Twidale, 1998; Bierman and Caffee, 2002). We suggest that variations in ^{10}Be concentrations within mildly deforming intraplate settings are unlikely to reflect climatic variability and may more likely provide a mechanism to distinguish between regions that have experienced recent tectonic activity from those which have not.

2. Study site

The Flinders Ranges are a geomorphically rugged, relatively high relief (up to 600–1000 m) uplands system in south-central Australia (Fig. 1). Although situated more than 2000 km from the closest plate boundary, the ranges define one of the most seismically active zones in Australia (Fig. 1), with hundreds of small earthquakes recorded annually and five magnitude >5.0 earthquakes recorded in the past century (Greenhalgh et al., 1994). Historical earthquake focal mechanisms indicate a roughly E–W oriented maximum principle compressive stress direction (Greenhalgh et al., 1994; Hillis and Reynolds, 2000; Clark and Leonard, 2003). The ranges are also bound by inward dipping reverse faults with Plio–Quaternary displacement histories. Investigations of these faults indicate (1) \sim E–W oriented paleo-maximum compressive stress orientations consistent with historical earthquakes, (2) Pliocene to Recent slip rates of 20–150 m/Myr (Sandiford, 2003; Quigley et al., 2006), and (3) episodic fault behaviour, with most recent surface displacements ranging from $\sim 12 \text{ ka}$ to ≥ 80 –100 ka (Quigley et al., 2006). A wealth of geologic evidence including fault data, regional Miocene–Pliocene unconformities, uplifted Miocene limestones, terminal Miocene changes in plate boundary kinematics and plate-scale numerical modelling imply that the presently active tectonic regime may be extrapolated back to at least ~ 5 –10 Ma and that tectonic uplift within this regime plausibly accounts for more than 50% of the present-day relief between range

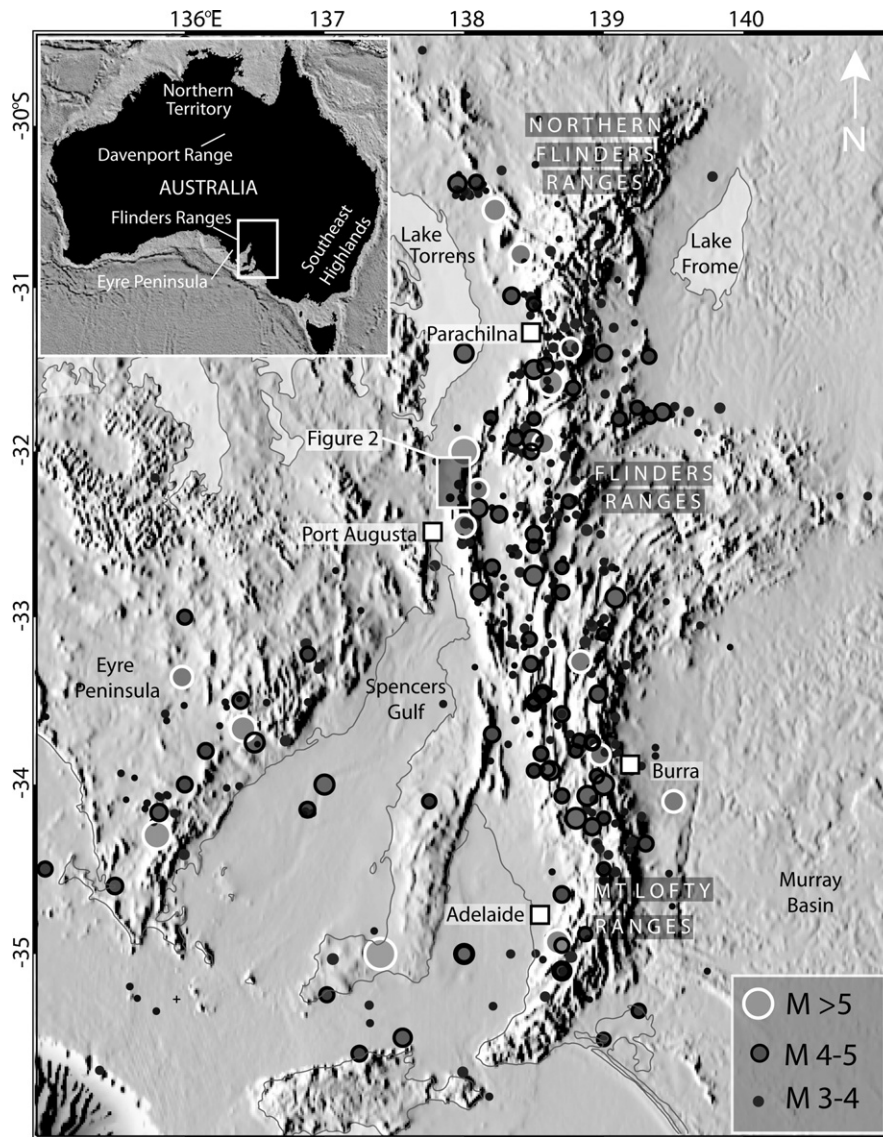


Fig. 1. Locations of earthquake epicenters in South Australia superimposed on a regional digital elevation map, showing spatial overlap of historical seismicity with the Flinders and Mount Lofty Ranges (Celerier et al., 2005). Earthquake epicenter data courtesy of Geoscience Australia. Magnitude measures are based on local magnitude (M_L) for $M < 5.5$ and surface magnitude (M_S) for $M > 5.5$. Inset shows correlation between principle compressive stress orientations derived from historical and pre-historic (neotectonic) datasets (Quigley et al., 2006). Location of Fig. 2 as shown.

tops and bounding piedmont surfaces (Sandiford, 2003; Sandiford et al., 2004; Quigley et al., 2006).

Several characteristics of the Flinders Ranges make them an ideal site for studying the connections between intraplate tectonism, ^{10}Be concentrations, and relief production. Firstly, the ranges are small relative to many of the world's intracontinental mountain belts, with a characteristic width of 50 km and an average relief of 500 m. Range bounding catchments have characteristically small sediment fluxes characterized by transport

distances from sediment source to sink of less than 10 km, an order of magnitude less than flexural length-scale of the lithosphere. Collectively these properties imply that any contribution of isostatic uplift of rocks in response to surface denudation is limited. Secondly, excellent exposures of range bounding faults and alluvial sequences permit regions subjected to young tectonic activity to be identified and compared to regions that have remained tectonically quiescent over late Quaternary timescales. The Wilkatana study area in

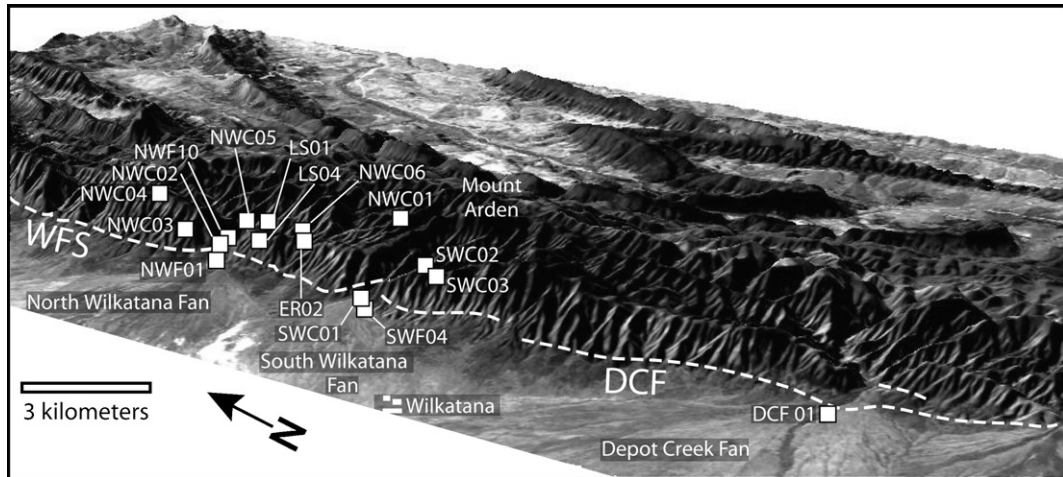


Fig. 2. ASTER satellite image and underlying digital elevation map (3× vertical exaggeration) of the Wilkatana area, looking east-northeast (Quigley et al., 2006). Location of ^{10}Be sample sites, Wilkatana Fault System (WFS) and Depot Creek Fault (DCF) as shown.

the central Flinders Ranges provides a site where well-established neotectonic gradients may be quantitatively investigated using ^{10}Be concentrations.

3. Geology of the Wilkatana area

The Wilkatana catchments are situated roughly 50 km N of Port Augusta along the western flank of the central Flinders Ranges (Fig. 1). The catchments cover an area of more than 60 km² (Figs. 2 and 3). The bedrock geology consists of a sequence of Neoproterozoic to Cambrian sediments, with resistant, steeply-dipping quartzite and sandstone strike-ridges forming steep rocky ridges and limestone and shale units forming more rounded undulating landforms. The regional climate is semi-arid, with mean annual precipitation reflecting altitude, latitude and aspect, ranging from 250 mm/yr at Port Augusta to over 400 mm/yr on the high ridges between Wilkatana and Parachilna. Annual evaporation exceeds 2000 mm regionally and consequently catchments within the Wilkatana and Parachilna areas are dry and lack any permanent water bodies.

The Wilkatana area contains some of the youngest and most spectacular exposures of late Quaternary faulting in continental Australia. The anatomizing, north-trending Wilkatana Fault System defines the range front over a length of at least 14 km (Fig. 2) and is exposed at various sites within the North and South Wilkatana Catchments where Proterozoic bedrock has been thrust westward over Quaternary alluvium (Fig. 4) (Williams, 1973; Quigley et al., 2006). Using combined structural analysis and optically stimulated lumines-

cence dating studies of faulted and post-faulting sediment, Quigley et al. (2006) established a cumulative total of more than 12 m of hangingwall uplift along the Wilkatana Fault System at North Wilkatana in response to three surface-rupturing earthquakes from ~67 to 12 ka, and estimated ~6 m of uplift along the fault at South Wilkatana since ~80 ka. The Wilkatana Fault System is marked by a 4–5 m high scarp along the range front immediately south of South Wilkatana (Fig. 5a) that diminishes in offset further south over a distance of several kilometers. The subsurface Depot Creek Fault (Fig. 2) appears to be a separate structure. The inferred surface projection of the Depot Creek Fault is blanketed by unfaulted alluvium that yielded a luminescence age of 71 ± 7 ka, indicating that this fault has not incurred a surface rupture event since this time (Quigley et al., 2006). The magnitude and frequency of late Quaternary reverse faulting and associated catchment uplift thus appears to decrease from north to south along the Wilkatana range front (Quigley et al., 2006).

The Wilkatana range front is one of the steepest and most linear range fronts in the Flinders Ranges (Fig. 2). Range-front slopes commonly exceed 20° between piedmonts and crests and we obtained an estimate of ~1.36 for the range-front sinuosity (Bull and McFadden, 1977). In comparison, range-front slopes in the Parachilna area of the Flinders Ranges to the north (Fig. 1) range from 5 to 10° with a sinuosity estimate of 2.19. Relatively unweathered and unvegetated landslide scars are present throughout the length of the range front, implying that landsliding plays an active and important role in the landscape response of this region. The most prominent and unvegetated landslide scar

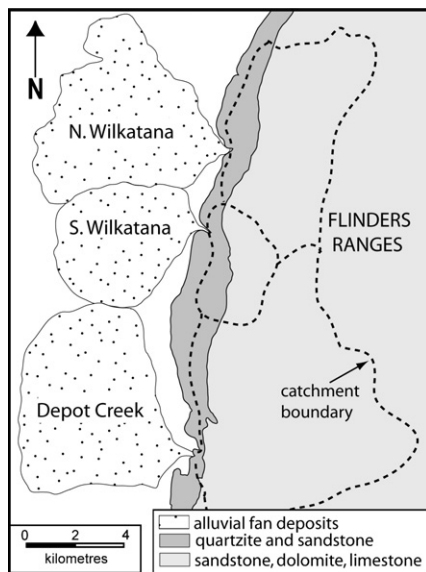


Fig. 3. Simplified geologic map of the Wilkatana alluvial fans and their source catchments.

occurs between the North and South Wilkatana Catchments (Fig. 5b), where as much as 5 m of fractured bedrock has been removed normal to the paleo-hillslope in the hangingwall of the Wilkatana Fault.

The Wilkatana alluvial fans are amongst the largest in Australia (Williams, 1973), covering an area of $>120 \text{ km}^2$ (Figs. 2 and 3). They comprise interbedded debris-flow deposits and clast-supported river gravels of Pliocene to Quaternary age (Williams, 1973). A 1–2 m thick calcareous paleosol capping fan surfaces is $\sim 25\text{--}35 \text{ ka}$ old (Williams, 1973). The fans have been dissected at their apexes to depths of 10–15 m and subsequently infilled by a sequence of Holocene to Recent alluvial gravels (Williams, 1973). Quigley et al. (in review) suggested that the volumetric accumulation of sediment in the Wilkatana fans relates to the focusing of neotectonic deformation in the Wilkatana area, while the transition from debris-flow to conglomeritic fan sedimentation at $\sim 30 \text{ ka}$ reflects a climatically-induced change from a soil-mantled to bedrock landscape in the source catchments. Holocene aggradation and dissection events were interpreted to reflect recurrence intervals of large magnitude floods capable of episodically transporting course catchment-derived sediment to the range front.

Hillslopes within the Wilkatana catchments consist of steep rock-mantled slopes containing abundant landslide scars and scree-slope deposits (Fig. 5c,d). Hillslopes commonly display sharp, highly convex profiles where v-shaped valleys are steeply incised into broader, u-shaped

valley forms, developed both in resistant and non-resistant lithologies. At some locations, colluvial deposits have encroached over top of creek beds, indicating that hillslope profiles are at maximum threshold steepness and are graded at least to the present creek base level (Fig. 5d). Creek valley floors consist of boulder-strewn stream beds with numerous bedrock strath surfaces. Bedrock floored valley exposures are generally restricted to quartzite and sandstone lithologies.

Late Quaternary tectonic activity appears to have influenced catchment geomorphology in several ways. By generating bedrock knickpoints where faults intersect stream systems (Fig. 4), stream gradients and therefore stream power have been increased as a result of tectonic uplift. Subsequent knickpoint propagation through the catchments provides a mechanism to explain ‘oversteepened’ catchment hillslopes and talus slopes that encroach onto stream beds. We also hypothesize that co-seismic ground shaking may have led to landsliding on catchment hillslopes, thus episodically increasing sediment yield from hillslopes in close proximity to the earthquake region, as observed in other settings (Dadson et al., 2004). Given that numerous landslides are apparent both along the range front between the North and South Wilkatana Catchments and within the North Wilkatana Catchment, the large late Quaternary paleoseismic events documented by Quigley et al. (2006), with moment magnitude estimates >6.6 and likely epicentral depths of $<10\text{--}20 \text{ km}$ (Greenhalgh et al., 1994), provide a mechanism to explain these features. In order to quantify the extent to which variations in late Quaternary tectonic uplift in the study area influenced catchment erosion rates, relief production and summit surface elevations, we measured ^{10}Be concentrations in bedrock and alluvial sediment.

4. Cosmogenic nuclide determinations of erosion rates

4.1. Methods

Bedrock samples were obtained by chiselling the uppermost few cm’s of quartz-bearing lithologies off subhorizontal bedrock outcrop surfaces. Stream sediment samples were collected from active stream channels by marking off a small ($<1 \text{ m}$ diameter) area and obtaining $\sim 3\text{--}5 \text{ kg}$ of mixed clast types and grain size from the sample site. Sampled grain size ranged from $<3 \text{ cm}$ in diameter to sand-sized grains. The entire sample was then crushed and the 90 to $250 \mu\text{m}$ diameter fraction was separated and analysed. This method was used to provide a well-mixed isotopic inventory of the catchment material irrespective of grain size. In a

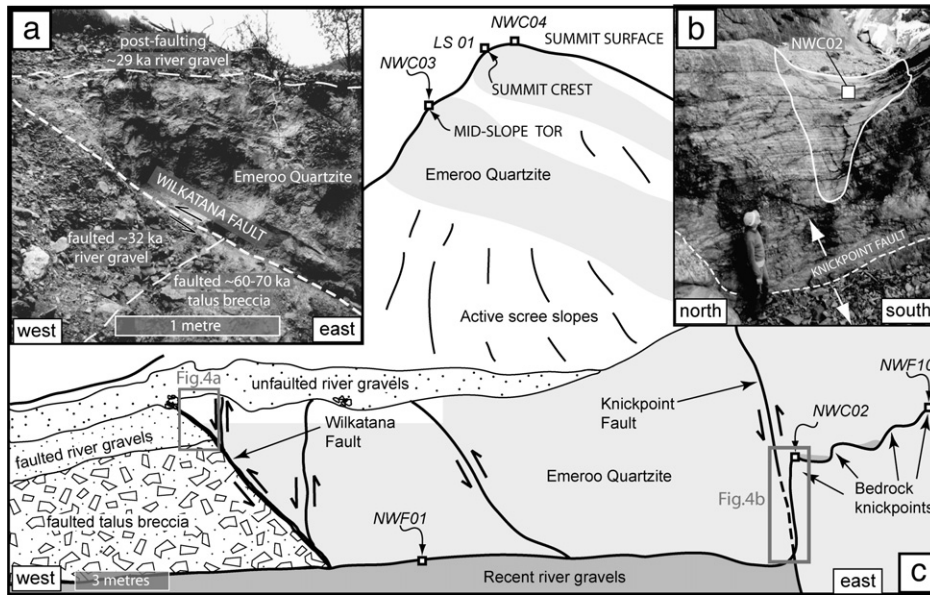


Fig. 4. (a) Field photograph of the Wilkatana Fault, showing structural–stratigraphic relationships described in text (Quigley et al., 2006). (b) Field photograph of the Knickpoint Fault, looking upstream into the North Wilkatana Catchment. Location of ^{10}Be sample NWC 02 within incised bedrock channel in fault hangingwall as shown. (c) Schematic cross-sectional sketch of the North Wilkatana Catchment at the range front, showing the location of fault exposures (a) and (b) and locations of bedrock knickpoints upstream of the knickpoint fault. Locations of stream sediment (NWF 01), valley floor (NWC02, NWF10), midslope (NWC 03) and summit surface (NWC 04) ^{10}Be sample sites as shown. Location of summit crest sample (LS 01) is projected onto the cross-section from the actual sample site to the south.

number of catchments, it has been shown that river sediment ^{10}Be concentrations show an inverse relationship with grain size, reflecting the different physical mechanisms responsible for generating and transporting material of different sizes (Brown et al., 1995; Matmon et al., 2005). However, no grain size dependence has been demonstrated in any of the arid region catchments measured so far (Granger et al., 1996; Clapp et al., 2000).

Field measurements of topographic shielding, sample thickness, and elevation were used to determine ^{10}Be production rates for bedrock samples. Catchment-averaged shielding and elevations were determined for the Wilkatana catchments from digital elevation maps and production rates were determined following the methods of Bierman and Steig (1996) and Binnie (2004). We used a reference ^{10}Be cosmogenic nuclide production rate at sea-level and high latitude of 5.1 ± 0.3 atoms $\text{g}^{-1} \text{yr}^{-1}$ (Stone, 2000). Samples for ^{10}Be measurement were prepared using standard methods (Kohl and Nishiizumi, 1992) and $^{10}\text{Be}/^9\text{Be}$ isotopic ratios were measured by accelerator mass spectrometry on the 14UD accelerator at the Australian National University (Appendix A).

Bedrock sample sites were selected on the basis of local geomorphic observations. Summit surface samples

(NWC 04, ER 02, SWC 02) were collected from subhorizontal bedrock surfaces displaying evidence of cm- to mm-scale exfoliation (Fig. 5e) and granular disintegration. NWC 01 and LS 01 were collected from bedrock outcrops at the break-in-slope between hilltops and hillslopes. Midslope samples (LS 04, NWC 03) were collected from the top surfaces of in situ, quartzite bedrock tors extending above the surrounding hillslope colluvium. We chose surfaces with abundant desert varnish that showed evidence for cm-scale exfoliation for sampling, although we were unable to find surfaces that demonstrated the same degree of varnish and weathering as observed at summit surfaces. This is interpreted to indicate faster rates of erosion on hillslopes. Since hillslope erosion is largely dominated by cobble-scale spallation and transport through talus slope deposits in this area, we inferred that ^{10}Be concentrations in these samples reflect a combination of steady-state cm-scale exfoliation and more sporadic, 10's of cm-scale rock fall events. Fluvial strath terrace samples (NWF 10, NWC 02, 05, 06) were collected from bedrock surfaces containing fluvial polish and fluted/grooved channels implying abrasion-dominated fluvial incision. We purposely avoided strath surfaces where evidence for recent plucking of coarse material larger than 5–10 cm was observed. Sites at elevations at

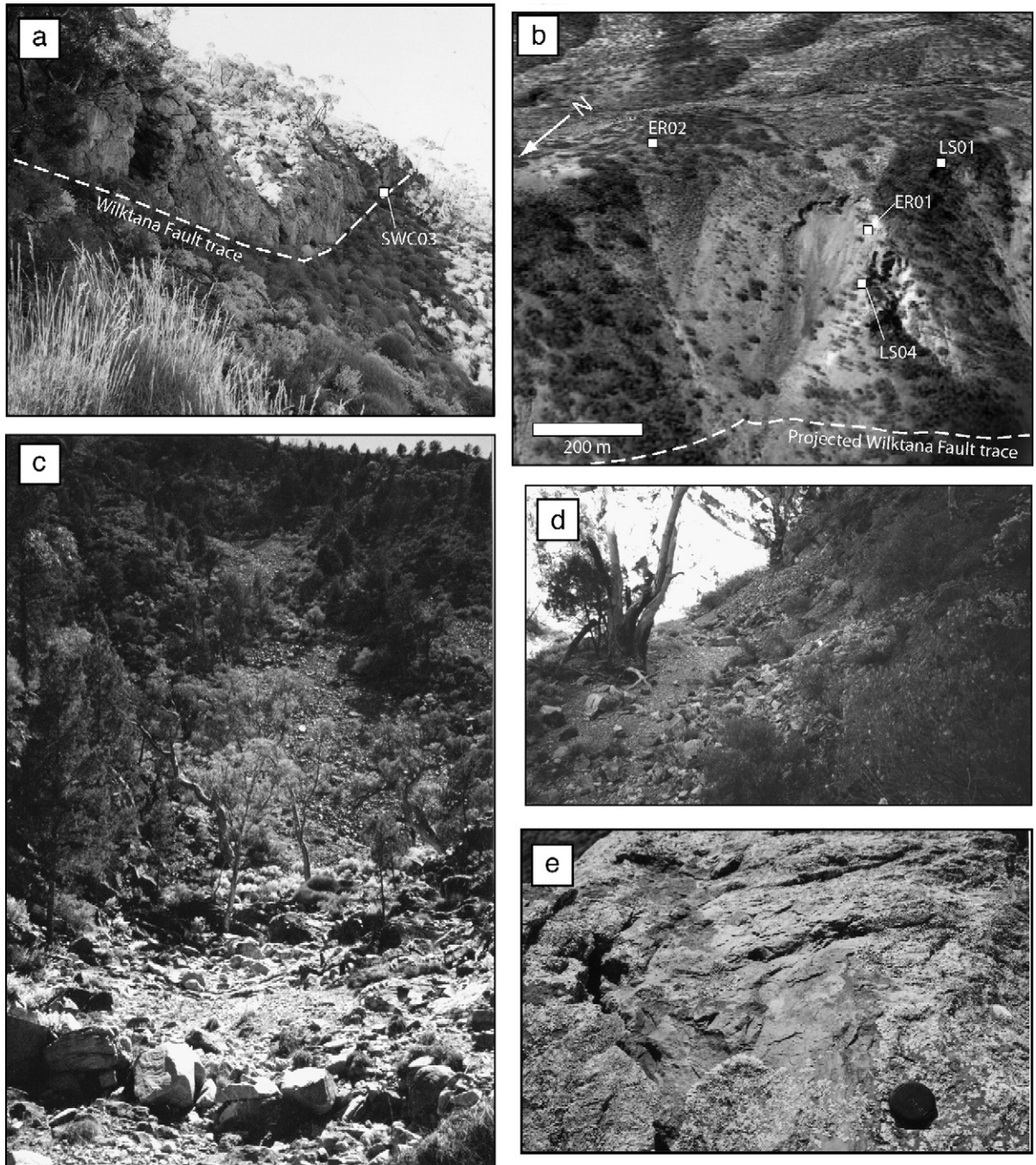


Fig. 5. (a) Field photograph of the Wilkatana Fault scarp south of the Wilkatana catchment, looking south. Location of ^{10}Be sample site SWC 03 as shown. (b) Aerial view of the range-front landslide that was dated using ^{10}Be analysis of sample ER01. Location of other sample sites and inferred position of the Wilkatana Fault as shown. Photo courtesy of Google Earth™. (c) Field photograph of the North Wilkatana Catchment, looking upstream to the northeast. Note abundant scree deposits on hillslopes and large accumulations of boulders along stream bed. (d) Field photograph of toe of scree deposit that has aggraded out into active stream bed. This relationship indicates scree slopes are graded to the modern stream channel and are actively contributing coarse sedimentary material into the catchment system. (e) Example of exfoliation-style weathering observed on summit surfaces targeted for ^{10}Be analysis. Sample SWC 02 was collected from this site.

or above locally preserved fluvial terraces were selected, where present, to minimize the possibility that straths underwent complex histories of alternating burial and exposure events (Fig. 4). Stream sediment samples (NWF 01, SWF 04, SWC 01 and DCF 01) were collected from the modern stream channels at the mouth of the Wilkatana catchments. SWF 04 was collected from stream sediment adjacent to the Wilkatana fault, roughly 100 m upstream of SWC 01. ^{10}Be concentrations in stream sediment reflect spatially-averaged erosion rates for quartz-bearing lithologies within each catchment (Bierman and Steig, 1996; Granger et al., 1996).

SWC 03 was collected from a striated fault surface at the base of the Wilkatana Fault System fault scarp roughly 4 m below the uplifted hangingwall surface, i.e. below the cosmogenic accumulation depth (Fig. 5a). Because this surface does not appear to have been eroded following faulting, the CN concentration in this sample reflects ^{10}Be acquired subsequent to faulting and therefore is interpreted as an exposure age. Finally, ER01 was collected from a steeply dipping, weakly striated surface marking the detachment surface of the major range-front landslide (Fig. 5b). The surface is interpreted to have been rapidly exposed from beneath the cosmogenic accumulation depth during a landslide that removed several meters of bedrock. We interpret the CN concentration in this sample to reflect the ^{10}Be acquired subsequent to landsliding, and to therefore provide a measure of the age of the landslide.

4.2. Results

Bedrock erosion rates at summit surfaces are relatively low ($\sim 5\text{--}10$ m/Myr) and increase slightly towards hillslope crests ($\sim 11\text{--}21$ m/Myr) (Appendix A). Hillslope erosion rates ($\sim 17\text{--}79$ m/Myr) and stream bottom incision rates ($\sim 58\text{--}123$ m/Myr) are significantly higher. Lowest ^{10}Be concentrations occurred within the recently uplifted bedrock channels in the hangingwall of the Knickpoint Fault (NWC 02 and NWF 10; Appendix A, Fig. 4) although corrections for the significant topographic shielding at these sites reduced erosion rate estimates to <100 m/Myr. ^{10}Be concentrations at all sites are interpreted to provide estimates of in situ denudation at given points in the landscape. In situ bedrock erosion rate estimates may either underestimate or overestimate long-term erosion rates (Small et al., 1997), however by sampling surfaces that show evidence for in situ weathering at short length scales (i.e. cm scale exfoliation and fluvial abrasion) we have attempted to sample sites that have not been subjected to recent large block

spallation or plucking that might result in overestimating long term rates. We are therefore confident that summit and hillslope samples provide reasonable proxies for long-term erosion rates, with the possibility that these in situ rates may even slightly underestimate long-term rates (Niemi et al., 2005). Bedrock knickpoint ^{10}Be concentrations measured within the North Wilkatana Catchment are more difficult to assess given the observed variability. Variations in knickpoint ^{10}Be concentrations could reflect either non-uniform knickpoint exposure histories (i.e., some knickpoints may have incurred episodic, short-lived burial by river sediment), unrecognized recent plucking events that resulted in lower ^{10}Be concentrations in exposed surfaces, or variable erosion due to slight variations in lithology. We therefore interpret valley floor ^{10}Be concentrations to provide broad constraints on the range of stream incision rates within the North Wilkatana Catchment, but note that these rates are nonetheless an order of magnitude higher than estimates of summit surface erosion.

Catchment-averaged erosion rates vary significantly (from ~ 6 to 49 m/Myr) between the three catchments (Appendix A). The North Wilkatana Catchment (NWF 01) yields the highest rate with a value intermediate between in situ hilltop, hillslope and valley floor erosion rates, consistent with the assumption that the contemporary stream sediment reflects a well-mixed spatial distribution of catchment material and that this erosion rate estimate is robust. The South Wilkatana Catchment yields the lowest erosion rates (SWC 01, 01R, SWF 04) with rates of $\sim 6\text{--}14$ m/Myr. The higher rate was obtained from the South Wilkatana streambed adjacent to the Wilkatana Fault while the lower rates were obtained roughly 100 m downstream of this site. We suspect that these ^{10}Be -derived rates provide an estimate of expected variability in ^{10}Be concentrations within alluvial sediment in this catchment. The Depot Creek Catchment (DCF 01) yields an intermediate rate of ~ 26 m/Myr. As similar sized particles of well-mixed lithologies were obtained from similar streambed locations in each sample site, we consider it unlikely that variations in sampled material or sample site induced the observed variation in erosion rate. The observed variability is also unlikely to reflect climatic conditions, catchment lithology or degree of vegetative cover, all of which are relatively uniform throughout the study area. Erosion rates also show no systematic relationship with catchment area (Table 1). In a general sense, the catchment displaying evidence for the youngest and most intense neotectonic activity yields the most rapid erosion rate. However the Depot Creek erosion rate is higher than the South Wilkatana erosion

Table 1
Morphologic and volumetric parameters from the Wilkatana alluvial fans and source catchments

Alluvial fan and source catchment	Fan volume (km ³)	Converted to rock volume (km ³)	Source catchment area (km ²)	Source catchment volume (km ³)	Time of fan sedimentation (Myr)	Catchment erosion rate (m/Myr)
North Wilkatana	1.169	0.831	16.5	4.18	4.71	10.7
South Wilkatana	0.617	0.439	8.4	2.09	4.71	11.1
Depot Creek	1.424	1.013	39.5	4.22	4.71	5.4

Fan areas were measured from ASTER imagery and volumes were obtained using fan depth constraints from drillhole and geophysical datasets (Preiss and Faulkner, 1984). Fan volumes were converted to rock volumes assuming a compacted fan density of $\rho = 1.97 \text{ g/cm}^3$ (Preiss and Faulkner, 1984) and rock density of $\approx 2.77 \text{ g/cm}^3$. Catchment areas and volumes were obtained using RiverToolsTM analysis of digital elevation models. Temporal constraints on fan deposition were obtained by correlating drillhole stratigraphy with comparative regional stratigraphic packages of known or inferred age. Catchment erosion rates are defined as the average rate of bedrock mass loss integrated over the entire catchment area (Matmon et al., 2005). For these calculations, we assumed closed system behaviour for the Wilkatana Fans e.g., (Allen and Hovius, 1998).

rate despite an apparent absence of post 70 ka neotectonic activity in the former. These relationships are explored in more detail in the Discussion.

The exposure age obtained from the Wilkatana Fault scarp indicates that this scarp formed in response to a large earthquake at $74 \pm 10 \text{ ka}$ (Appendix A). This is consistent with the interpretation that a large earthquake occurred at the mouth of the South Wilkatana Catchment at $\leq 80 \text{ ka}$, generating $\sim 6 \text{ m}$ of offset at this time (Quigley et al., 2006). The exposure age obtained from the landslide site indicates that landsliding occurred at $14 \pm 3 \text{ ka}$ (Appendix A), coincident with last inferred motion on the Knickpoint Fault branch of the Wilkatana Fault (Quigley et al., 2006) (Fig. 2). This suggests that neotectonic faulting triggered landsliding that may have temporarily increased sediment input into the Wilkatana catchments.

5. Discussion

5.1. Spatial and temporal variability of erosion

In situ bedrock and catchment-averaged ¹⁰Be erosion rates provide insight into the late Quaternary geomorphic evolution of the Wilkatana catchments. ¹⁰Be data from the North Wilkatana Catchment indicate late Quaternary increases in relief because summit surface erosion rates are exceeded by hillslope and valley floor erosion rates and catchment-averaged erosion rates. The difference between summit surface and valley floor erosion rates indicates a relief production rate of $\sim 47\text{--}118 \text{ m/Myr}$. Since in situ hillslope and valley floor data were not obtained from the other catchments, considerably more caution is required in deducing relief production histories for these catchments. In the Depot Creek Catchment, catchment-averaged rates exceed summit surface lowering rates implying either late Quaternary increases in catchment relief and/or sedi-

ment supply, albeit to a much lesser degree than in the North Wilkatana Catchment. Conversely, catchment-averaged erosion rates in South Wilkatana are roughly equivalent to summit surface erosion rates. This suggests that the ¹⁰Be flux from this catchment is in equilibrium with summit erosion, as might be expected from a ‘steady-state’ landscape undergoing uniform lowering.

Further insight into the geomorphic development of the Wilkatana catchments is obtained by comparing ¹⁰Be catchment-averaged erosion rates with longer-term estimates of erosion obtained from mass balance calculations of Plio–Quaternary sediment deposited within the Wilkatana alluvial fans (Table 1). Details of this method are provided in the Table 1 caption. Long-term catchment-averaged erosion rates are significantly slower than the ¹⁰Be rates for the North Wilkatana and Depot Creek Catchments and consistent with ¹⁰Be rates for the South Wilkatana Catchment. This relationship suggests that the sediment flux from the North Wilkatana and Depot Creek Catchments has increased in the late Quaternary relative to longer-term rates. However, the sediment flux from the South Wilkatana Catchment suggests that ¹⁰Be release catchment is currently in equilibrium with the longer-term sediment yields.

Several aspects of the North Wilkatana Catchment may account for the anomalously low ¹⁰Be concentrations relative to the other catchments. This catchment incurred at least three surface-rupturing earthquakes since $\sim 67 \text{ ka}$, including a young event at $\sim 12 \text{ ka}$, that were not recognized in adjacent catchments. Fault-generated knickpoints developed in stream profiles and increased stream gradients, thereby providing a mechanism for increased rates of stream incision and transport of low ¹⁰Be material through this catchment relative to adjacent catchments. The concentration of neotectonic activity proximal to the North Wilkatana

Catchment also implies that co-seismic ground shaking and resultant liberation of low ^{10}Be material from proximal hillslopes via landsliding would have been more pronounced in this catchment relative to adjacent catchments during seismic events. Peak ground velocities associated with strong, near-fault ground motions scale, to a first approximation, with the reciprocal of the square root of distance from the fault plane (Mavroëidis and Papageorgiou, 2003), implying that peak ground motions generated along the relevant ~ 10 km section of the Wilkatana range front could vary by as much as a factor of 3 for an individual event. In support of this hypothesis, the $\sim 14.3 \pm 3.1$ ka age of the range-front landslide is consistent with independent evidence for the Knickpoint Fault event at ~ 12 ka, implying that this seismic event triggered mass wasting on hillslopes. We note that ^{10}Be -derived denudation rates in other settings also appear to increase with proximity to active fault scarps (Riebe et al., 2001a,b; von Blanckenburg, 2006) suggesting a similar relationship to that observed here. In the periods where material generated by seismic shaking on steep slopes dominates the stream sediment flux, and in the immediate aftermath of such events, ^{10}Be concentrations will likely be significantly lower than the long-term average (Niemi et al., 2005). The characteristic response time of the ^{10}Be system to re-establish to the longer-term (or background) concentration will be inversely proportional to the background erosion rate. The contemporary sediment mass has an effective memory of the erosion history over the time interval required to erode to the characteristic depth for cosmogenic production (typically about 0.6 m). For background erosion rates of the order of 10 m/Myr, appropriate to the Wilkatana catchments, the sediment carries an effective memory of the erosion on the 10–100 kyr timescale, with a characteristic response time following an episodic massive, sediment release event estimated at ~ 50 kyr. We thus conclude that the North Wilkatana Catchment is in a state of cosmogenic disequilibrium in response to neotectonic activity and coeval landsliding.

The significantly higher ^{10}Be concentrations in South Wilkatana alluvium suggest that either the processes that led to an increased abundance of low ^{10}Be material in the North Wilkatana Catchment were less pervasive, or that the South Wilkatana Catchment re-equilibrated to background erosional conditions more rapidly. We are unable to quantitatively distinguish between these hypotheses, but note that many hillslopes within the South Wilkatana Catchment are dominated by in situ bedrock and contain fewer talus deposits and landslide scars than North Wilkatana. This suggests that

co-seismic shaking and input of low ^{10}Be material into this catchment was less pervasive than in the North Wilkatana Catchment. We suggest that an increased distance from neotectonic epicenters, and perhaps unrecognized lithologic variability, provide plausible explanations to explain this relationship.

The Depot Creek Catchment is farthest away from the concentrated neotectonic activity exposed in North Wilkatana. In addition the Depot Creek Fault appears to have been inactive since ~ 74 ka. This suggests that co-seismic ground motion in this catchment is likely to have been less pervasive than in the North and South Wilkatana Catchments. We offer two explanations for why the Depot Creek alluvium yields lower ^{10}Be concentrations than South Wilkatana. Firstly, as the largest and most lithologically variable catchment, it is plausible that tectonic knickpoints generated from pre 74 ka faulting have propagated farther into the Depot Creek Catchment than in South Wilkatana. This could result in more pervasive hillslope over-steepening and increased susceptibility of hillslopes to mass wasting despite similar or lesser magnitudes of co-seismic ground shaking, particularly in less resistant lithologies. Secondly, it is possible that low ^{10}Be hillslope material has been more effectively stored within the Depot Creek Catchment relative to the small, steep South Wilkatana Catchment. In this scenario, modern flood events continue to transport remnants of low ^{10}Be mass wasting deposits from the Depot Creek Catchment while similar deposits have already been effectively flushed from the smaller South Wilkatana Catchment.

5.2. Constraining surface uplift

^{10}Be point measurements of bedrock erosion rate can be combined with estimates of post ~ 80 ka bedrock tectonic uplift along the Wilkatana Fault to quantify the vertical displacement of bedrock surfaces relative to a horizontal datum, in this case, the piedmont surfaces that bound the range front. Using the relation that surface uplift of ranges relative to piedmont is given by the tectonic uplift of bedrock relative to piedmont minus the bedrock erosion (e.g., England and Molnar, 1990) we converted ^{10}Be erosion rates into erosion magnitudes in order to quantify the amount of bedrock erosion since ~ 80 ka, and assumed that sub-horizontal summit surfaces throughout the study area erode at the range of rates indicated from the ^{10}Be data. These calculations indicate that summits may have been uplifted by > 11 m relative to the bounding piedmont in the North Wilkatana Catchment since ~ 80 ka due to movement along the Wilkatana Fault (Table 2). Conversely, summit

Table 2
Estimates of post 80 ka surface uplift in the Wilkatana area

Catchment	Bedrock uplift (m)	Summit erosion (m)	Valley incision (m)	Summit surface displacement (m)	Valley floor displacement (m)
North Wilkatana	≥ 12.0	0.4–0.8	4.7–9.8	11.2–11.6	2.2–7.3
South Wilkatana	≥ 6.0	0.4–0.8	–	5.2–5.6	–
Depot Creek	0–6.0	0.4–0.8	–	–0.8–5.6	–

surfaces may have experienced a net lowering of <1 m relative to the bounding piedmont in the Depot Creek Catchment over this time, since no evidence for post ~80 ka tectonic uplift was observed there. Stated simply, these data indicate that late Quaternary tectonism led to mountain surface uplift in parts of the Flinders Ranges because tectonic uplift outpaced summit surface erosion at these sites.

Measurements of bedrock incision rate were also combined with tectonic uplift magnitudes to track the vertical path of valley floors in the North Wilkatana Catchment (Table 2). The data indicate that valley floors have incised a similar, but slightly lesser magnitude than tectonic uplift and therefore have been vertically uplifted ~2–7 m relative to bounding piedmonts. We interpret this data, together with field observations, to

indicate that the North Wilkatana Catchment is presently in a state of geomorphic disequilibrium as it attempts to respond to late Quaternary tectonic activity via increased rates of valley incision.

5.3. ^{10}Be concentrations, intraplate tectonism and climate change

Fault behaviour in mildly deforming intraplate settings is commonly episodic on both the temporal and spatial scale (Crone et al., 1997, 2003). This suggests that continental plate interiors are comprised of a mosaic of landscapes in varying states of response to tectonism, with some landscapes responding to recent (even historical) tectonic activity and other landscapes removed from tectonic events for ≥100 k.y. In the

Table 3
Summary of ^{10}Be erosion rate estimates and climate data from other Australian sites

Location	Reference	Sample type (# analyses)	Average ^{10}Be erosion rate (m/Myr) ^a	Mean annual rainfall (mm)
Eyre Peninsula	Bierman and Caffè (2002)	Bedrock inselbergs (68)	1.3±0.2	325
Northern Territory	Bierman and Caffè (2002)	Bedrock inselbergs (19)	2.2±0.3	1128
Davenport Ranges	Belton et al. (2004)	Bedrock surfaces (10)	2.1±0.3	316
Northern Territory	Nott and Roberts (1996)	Contemporary stream sediment ^b	3.6±1.4	1128
Southeast highlands	Heimsath et al. (2001)	Contemporary stream sediment(2)	15.9±1.2	500–700
Southeast highlands	Heimsath et al. (2001)	Bedrock fluvial straths (4)	9.9±0.7	500–700
Southeast highlands	Heimsath et al. (2001)	Bedrock torrs (10)	10.0±0.8	500–700
Southeast highlands	Heimsath et al. (2001)	Bedrock surfaces (2)	22.6±1.7	500–700
Northern Flinders Ranges	Quigley et al. (2007)	Bedrock summit surfaces (2)	14.2±1.4	254
Northern Flinders Ranges	Quigley et al. (2007)	Bedrock hillslope surfaces (4)	22.7±3.0	254
Northern Flinders Ranges	Quigley et al. (2007)	Alluvium (1)	22.8±2.8	254
Brachina area	Bierman et al. (1998)	Bedrock surfaces (2)	3.0±1.0	313
Brachina area	Bierman et al. (2002)	Piedmont surfaces (3)	2.7±0.9	313
Parachilna area	Heimsath and Chappell, person commun	Bedrock surfaces (2)	10.0±5.0	313

^a Average rate and error for given sample numbers.

^b # analyses, ^{10}Be production rate not reported.

absence of neotectonic fault exposures, it may be difficult to determine which parts of landscapes have been influenced by recent tectonism and which have not. In this study, we conclude that anomalously low ^{10}Be concentrations in hillslope and valley floor bedrock samples and alluvial sediment in the North Wilkatana Catchment reflect recent (i.e. last ~ 50 k.y.) neotectonic forcing of landscape evolution with catchment-scale spatial variability. ^{10}Be concentrations from the North Wilkatana Catchment yield the highest recorded bedrock erosion rates in Australia. This suggests that anomalously low ^{10}Be concentrations may serve as a ‘tracer’ for neotectonic activity in other unglaciated mountain belts, including intraplate and plate boundary settings.

Our dataset is also pertinent to the debate over the roles of tectonics and climate in mountain erosion and relief production. If climate was the dominant control of alluvial ^{10}Be concentrations in the study area, we would expect that catchment erosion rates should be relatively constant within the region, given the lack of a climatic gradient between the proximal catchments. Given that the lowest alluvial ^{10}Be concentration occurs within the catchment most affected by recent neotectonic activity, we infer that recent tectonism led to an influx of low ^{10}Be concentration into this catchment. Other lines of evidence also suggest a minimal climatic influence on the rates of mountain erosion in this region. In the arid northern Flinders Ranges, where neotectonic activity has been demonstrated, ^{10}Be concentrations in subhorizontal granite bedrock summit surfaces indicate erosion rates of ~ 14 m/Myr (Table 3) (Quigley et al., 2007). In the humid Northern Territory of northern Australia, where neotectonic activity is sparse, ^{10}Be concentrations in subhorizontal granite bedrock surfaces indicate erosion rates of 2–4 m/Myr (Table 3). In the semi-arid Davenport Range, where neotectonic activity has not been recognized, ^{10}Be concentrations in quartzite bedrock surfaces indicate erosion rates of 0.3 m/Myr (Table 3) (Belton et al., 2004). The lack of a correlation between bare rock erosion rate and precipitation and positive correlation between bedrock erosion and neotectonic activity implies a tectonic, as opposed to climatic, influence on bedrock erosion rate. Furthermore, late Quaternary fluvial incision rates in the Flinders Ranges (50–220 m/Myr (reported herein and Quigley et al., 2007), are dramatically faster than ~ 9 m/Myr incision rates indicated from ^{10}Be concentrations in bedrock straths in the Bredbo River in the southeastern Australian Highlands (Table 3) (Heimsath et al., 2001). No evidence for late Quaternary surface rupturing is present in the latter region, implying that the stream incision rates acquired by (Heimsath et al., 2001)

provide reasonable proxy incision rates for a transient landscape not subject to recent tectonic forcing. We therefore infer that rates of bedrock river incision in the Wilkatana catchment have been strongly influenced by neotectonic processes such as knickpoint formation and migration, confirming the link between neotectonism, fluvial incision and relief production (e.g., Stock et al., 2005). Obviously, sediment transport in ephemeral streams such as in the Wilkatana catchments depends upon the recurrence of flood events with sufficient stream power to transport coarse bedload, however the recurrence of these events is relatively short ($\sim 1/1500$ yr) compared to the timescale of ^{10}Be accumulation.

Our results provide quantitative support for a youthful component to relief production in an intraplate mountain belt for which the age of relief is frequently debated. While it is uncertain how the rates apply to longer geologic timescales, the recognition that mildly deforming continental interiors may be subject to brief periods of tectonic rejuvenation, and that this signal may be detected using ^{10}Be is widely applicable to intraplate mountain belts around the world. This is particularly the case for continents such as Australia, which are commonly regarded as geomorphically and tectonically quiescent.

Acknowledgements

We thank Paul Bierman, Tom Gardner and several anonymous reviewers for their detailed and instructive comments on earlier drafts of this manuscript. Arjun Heimsath and John Chappell are thanked for access to unpublished data. This work has been supported by ARC Discovery grants DP0558705 and DP556133.

Appendix A. Supplementary data

Supplementary data associated with this article can be found, in the online version, at [doi:10.1016/j.epsl.2007.06.020](https://doi.org/10.1016/j.epsl.2007.06.020).

References

- Allen, P.A., Hovius, N., 1998. Sediment supply from landslide-dominated catchments; implications for basin-margin fans. *Basin Research* 10, 19–35.
- Belton, D., Brown, R., Kohn, B., Fink, D., Farley, K., 2004. Quantitative resolution of the debate over antiquity of the central Australian landscape: implications for the tectonics and geomorphic stability of cratonic interiors. *Earth and Planetary Science Letters* 219, 21–34.
- Bierman, P.R., Caffè, M., 2002. Cosmogenic exposure and erosion history of Australian bedrock landforms. *Geological Society of America Bulletin* 114, 787–803.

- Bierman, P., Steig, E., 1996. Estimating rates of denudation and sediment transport using cosmogenic isotope abundances in sediment. *Earth Surface Processes and Landforms* 21, 125–139.
- Bierman, P., Larsen, P., Clapp, E., Clark, D., 1996. Refining estimates of 10-Be and 26-Al production rates. *Radiocarbon*, v. 38, no. 1, p. 149. *Radiocarbon* 38, 149.
- Bierman, P., Albrecht, A., Bothner, M., Brown, E., Bullen, T., Gray, L., Turpin, L., 1998. Weathering, erosion and sedimentation. In: Kendall, C., McDonnell, J.J. (Eds.), *Isotope Tracers in Catchment Hydrology*, Chapter 23. Elsevier, pp. 647–678.
- Bierman, P.R., Caffee, M., 2001. Slow rates of rock surface erosion and sediment production across the Namib desert and escarpment, southern Africa. *American Journal of Science* 301, 3263–3258.
- Bierman, P., Caffee, M., Davis, P., Marsella, K., Pavich, M., Colgan, P., Mickelson, D., Larsen, J., 2002. Rates and timing of earth surface processes from in situ-produced cosmogenic Be-10. *Reviews in Mineralogy and Geochemistry* 50, 147–205.
- Binnie, S., 2004. Deriving basin-wide denudation rates from cosmogenic radionuclides, San Bernardino Mountains, California, unpublished PhD Thesis The University of Edinburgh. 330p.
- Brown, T.B., Stallard, R.F., Larsen, M.C., Raisbeck, G.M., Francoise, Y., 1995. Denudation rates determined from accumulation of in situ-produced 10Be in the Luquillo Experimental Forest, Puerto Rico. *Earth and Planetary Science Letters* 129, 192–202.
- Bull, W.B., McFadden, L.D., 1977. Tectonic geomorphology north and south of the Garlock Fault, California. In: Doehring, D.O. (Ed.), *Geomorphology in Arid Regions*. State University of New York at Binghamton.
- Callen, R.A., Tedford, R.H., 1976. New late Cainozoic rock units and depositional environments, Lake Frome Area, South Australia. *Transactions of the Royal Society of South Australia* 100, 125–167.
- Celerier, J., Sandiford, M., Hansen, D.L., Quigley, M., 2005. Modes of active intraplate deformation, Flinders Ranges, Australia. *Tectonics* 24. doi:10.1029/2004&C001679.
- Clapp, E.M., Bierman, P.R., Schick, A.P., Lekach, J., Enzel, Y., Caffee, M., 2000. Sediment yield exceeds sediment production in arid region drainage basins. *Geology* 28, 995–998.
- Clark, D.J., Leonard, M., 2003. Principal stress orientations from multiple focal plane solutions: new insight in to the Australian intraplate stress field. In: Hillis, R.R., Muller, D. (Eds.), *Evolution and Dynamics of the Australian Plate*. Geological Society Australia Special Publication, vol. 22, pp. 85–99.
- Crone, A.J., Machette, M.N., Bowman, J.R., 1997. Episodic nature of earthquake activity in stable continental regions revealed by palaeoseismicity studies of Australian and North American Quaternary faults. *Australian Journal of Earth Sciences* 44, 203–214.
- Crone, A.J., De Martini, P.M., M.M.N., Okumura, K., Prescott, J.R., 2003. Palaeoseismicity of two historically quiescent faults in Australia — implications for fault behaviour in stable continental regions. *Bulletin of the Seismological Society of America* 93, 1913–1934.
- Dadson, S.J., Hovius, N., Chen, H., Dade, W., Lin, J., Hsu, M., Lin, C., Hornig, M., Chen, T., Milliman, J., Stark, C., 2004. Earthquake-triggered increase in sediment delivery from an active mountain belt. *Geology* 32, 733–736.
- Dunne, J., Elmore, D., Muzikar, P., 1999. Scaling factors for the rate of production of cosmogenic nuclides for geometric shielding and attenuation at depth on sloped surfaces. *Geomorphology* 27, 3–12.
- England, P., Molnar, P., 1990. Surface uplift, uplift of rocks, and exhumation of rocks. *Geology* 18, 1173–1177.
- Granger, D.E., Kirchner, J.W., Finkel, R., 1996. Spatially averaged long-term erosion rates measured from in situ produced cosmogenic nuclides in alluvial sediment. *Journal of Geology* 104, 249–257.
- Greenhalgh, S., Love, D., Malpas, K., McDougall, R., 1994. South Australian earthquakes, 1980–92. *Australian Journal of Earth Sciences* 41.
- Heimsath, A.M., Chappell, J., personal communication.
- Heimsath, A.M., Chappell, J., Dietrich, W.E., Nishiizumi, K., Finkel, R.C., 2001. Late Quaternary erosion in southeastern Australia: a field example using cosmogenic nuclides. *Quaternary International* 83, 69–185.
- Hillis, R.R., Reynolds, S.D., 2000. The Australian stress map. *Journal of the Geological Society (London)* 157, 915–921.
- Kohl, C.P., Nishiizumi, K., 1992. Chemical isolation of quartz for measurement of in situ-produced cosmogenic nuclides. *Geochimica et Cosmochimica Acta* 56.
- Kuhlemann, J., Frisch, W., Dunkl, I., Székely, B., 2001. Quantifying tectonic versus erosive denudation by the sediment budget: the Miocene core complexes of the Alps. *Tectonophysics* 330, 1–23.
- Lal, D., 1991. Cosmic ray labeling of erosion surfaces: in situ production rates and erosion models. *Earth and Planetary Science Letters* 104, 424–439.
- Matmon, A., Bierman, P.R., Larson, J., Southworth, S., Pavich, M., Finkel, R.C., Caffee, M., 2005. Grain size dependency of 10Be concentrations in alluvial sediments in the Great Smoky Mountains, Grain size dependency of 10Be concentrations in alluvial sediments in the Great Smoky Mountains. *Geochimica et Cosmochimica Acta* 69.
- Macroceid, G.P., Papageorgiou, A.S., 2003. A mathematical representation of near-fault ground motions. *Bulletin of the Seismological Society of America* 93, 1099–1131.
- McMillan, M.E., Angevine, C.L., Heller, P.L., 2002. Postdepositional tilt of the Miocene–Pliocene Ogallala Group on the western Great Plains: evidence of late Cenozoic uplift of the Rocky Mountains. *Geology* 30, 63–66.
- Niemi, N.A., Oskin, M., Burbank, D.W., Heimsath, A.M., Gabet, E.J., 2005. Effects of bedrock landslides on cosmogenically determined erosion rates. *Earth and Planetary Science Letters* 237, 480–498.
- Nott, J., Roberts, R., 1996. Time and process rates over the past 100 m.y.: a case for dramatically increased landscape denudation rates during the late Quaternary in northern Australia. *Geology* 24, 883–887.
- Preiss, W.V., Faulkner, P., 1984. Geology, geophysics and stratigraphic drilling at Depot Creek, Southern Flinders Ranges. *Geological Survey of South Australia, Quaterly Notes* 89, 10–19.
- Quigley, M., Cupper, M., Sandiford, M., 2006. Quaternary faults of southern Australia: palaeoseismicity, slip rates and origin. *Australian Journal of Earth Sciences* 53, 285–301.
- Quigley, M., Sandiford, M., Fifield, K., Alimanovic, A., 2007. Bedrock erosion and relief production in the northern Flinders Ranges, Australia. *Earth Surface Processes and Landforms* 32, 929–944.
- Quigley, M., Sandiford, M., Cupper, M., in review. Distinguishing tectonic from climatic controls on range-front sedimentation, Flinders Ranges, South Australia, Basin Research.
- Riebe, C., Kirchner, J.W., Granger, D.E., Finkel, R.C., 2001a. Minimal climatic control on erosion rates in the Sierra Nevada, California. *Geology* 29, 447–450.
- Riebe, C.S., Kirchner, J.W., Granger, D.E., Finkel, R.C., 2001b. Strong tectonic and weak climatic control of long-term chemical weathering rate. *Geology* 29, 511–514.

- Riebe, C.S., Kirchner, J.W., Finkel, R.C., 2004. Erosional and climatic effects in long-term chemical weathering rates in granitic landscapes spanning diverse climate regimes. *Earth and Planetary Science Letters* 224, 547–562.
- Sandiford, M., 2003. Neotectonics of southeastern Australia: linking the Quaternary faulting record with seismicity and in situ stress. In: Hillis, R.R., Muller, D. (Eds.), *Evolution and Dynamics of the Australian Plate*. Geological Society of Australia Special Publication, vol. 22, pp. 101–113.
- Sandiford, M., Wallace, M., Coblentz, D., 2004. Origin of the in situ stress field in south-eastern Australia. *Basin Research* 16, 325–338.
- Small, E.E., Anderson, R.S., Repka, J.L., Finkel, R., 1997. Erosion rates of alpine bedrock summit surfaces deduced from in situ ^{10}Be and ^{26}Al . *Earth and Planetary Science Letters* 250, 413–425.
- Stock, G.M., Anderson, R.S., Finkel, R.C., 2005. Rates of erosion and topographic evolution of the Sierra Nevada, California, inferred from cosmogenic ^{26}Al and ^{10}Be concentrations. *Earth Surface Processes and Landforms* 30, 985–1006.
- Stone, J.O., 2000. Air pressure and cosmogenic isotope production. *Journal of Geophysical Research* 105B, 23753–23759.
- Twidale, C.R., 1998. Antiquity of landforms: an “extremely unlikely” concept vindicated. *Australian Journal of Earth Sciences* 45, 657–668.
- Twidale, C.R., Bourne, J.A., 1975. Geomorphological evolution of part of the eastern Mount Lofty Ranges, South Australia. *Transactions of the Royal Society of South Australia* 99, 197–209.
- Veevers, J.J., 1984. *Phanerozoic Earth History of Australia*. Oxford University Press, New York, p. 418.
- von Blanckenburg, F., 2006. The control mechanisms of erosion and weathering at basin scale from cosmogenic nuclides in river sediment. *Earth and Planetary Science Letters* 242, 224–239.
- Williams, G.E., 1973. Late Quaternary piedmont sedimentation, soil formation and palaeoclimates in arid South Australia. *Zeitschrift für Geomorphologie* 7, 102–125.
- Zhang, P., Molnar, P., Downs, W.R., 2001. Increased sedimentation rates and grain sizes 2–4 Myr ago due to the influence of climate change on erosion rates. *Nature* 410, 891–897.